

Visible Light-Mediated Photoactivated Sulfur Quantum Dots as Heightened Antibacterial Agents

Saurabh Shivalkar, Farwa Arshad, Amaresh Kumar Sahoo,* and Md Palashuddin Sk*

Cite This: *ACS Omega* 2022, 7, 33358–33364

Read Online

ACCESS |



Metrics & More

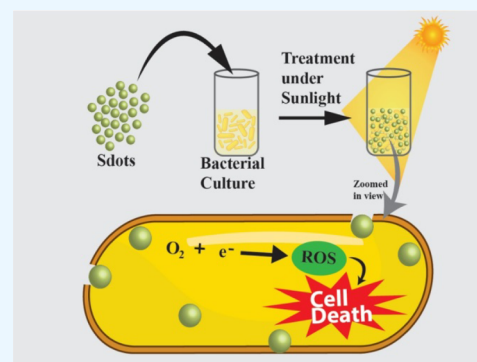


Article Recommendations



Supporting Information

ABSTRACT: The need for antimicrobial or antibacterial fabric has increased exponentially in recent past years, especially after the outbreak of the SARS-CoV-2 pandemic. Several studies have been conducted, and the primary focus is the development of simple, automated, performance efficient and cost-efficient fabric for disposable and frequent-use items such as personal protective materials. In this regard, we have explored the light-driven antibacterial activity of water-soluble Sdots for the first time. Sdots are a new class of non-metallic quantum dots of the nanosulfur family having a polymeric sulfur core. These Sdots exhibited excellent antibacterial activity by generating reactive oxygen species under sunlight or visible light. Under 6 h of sunlight irradiation, it was observed that >90% of the bacterial growth was inhibited in the presence of Sdots. Furthermore, low toxic Sdots were employed to develop antibacterial fabric for efficiently cleaning the bacterial infection. The prominent zone of inhibition of up to 9 mm was observed post 12 h incubation of Sdots treated fabric with *E. coli* in the presence of visible light. Furthermore, the SEM study confirmed the bactericidal effect of these Sdots-treated fabrics. Moreover, this study might help explore the photocatalytic disinfection application of Sdots in diverse locations of interest, Sdots-based photodynamic antimicrobial chemotherapy application, and provide an opportunity to develop Sdots as a visible light photocatalyst for organic transformations and other promising applications.



INTRODUCTION

Antimicrobial resistance is one of the prime concerns globally in the present decade, and the situation is aggravating gradually as bacteria can overcome the effects of antibiotics via genetic alterations.¹ The rapid adaptability of the hostile challenges of antibiotics by the numerous pathogenic bacterial strains is an impediment in subjugating the infections without developing a novel therapeutic.² Thus, bacterial infections continue to surge and lead to causes of death for millions of people annually.³ There is an urgent call to develop effective alternative strategies that may lead to raise multiple pathways for combating bacterial infections. In this regard, light-responsive nanostructures [semiconductor materials, g-C₃N₄, MoS₂, nanosheets, carbon dots (Cdots), etc.] are emerging as efficient and viable alternatives to conventional antibacterial agents.^{4–9} In the presence of light, either photogenerated electrons and holes or photogenerated electrons from these nanostructures participate in producing reactive oxygen species (ROS), which effectively contribute to the oxidative stress on the cell membrane, inhibiting the pathogenic bacteria by impairing the cell membrane. In most cases, these nanostructures have a high band gap, and their photo charge carriers also have a high redox potential. They show UV light-activated antibacterial effect.^{10–12} However, commonly proposed light-sensitive metallic nanostructures/semiconducting quantum dots could not produce the expected outcomes, owing to their toxicity and non-biocompatibility.^{13–16} Hence, fabricating a potent

photoactivated antibacterial agent using these metallic/semi-conducting nanostructures limits their implementation for in vivo applications. Therefore, the visible light-activated non-toxic (or less toxic) antibacterial agent is an excellent solution for real-life applications.^{17–19} In addition, visible light-mediated bacterial death is appropriate for diverse locations of interest as any place can be pathogen-free by providing light-emitting diode light or sunlight.

Non-metallic quantum dots such as Cdots are explored for photoactivated antibacterial effects.^{9,20} Recently, another non-metallic quantum dot of the nanosulfur family named sulfur quantum dots (Sdots) has emerged as a new class of non-toxic (or less toxic) fluorescent material.^{21–23} Sdots consist of a polymeric sulfur core and exhibit exciting photophysical properties.²⁴ Sdots have been employed for photoluminescence-related versatile applications.^{21–23} Nanoscale sulfur (not Sdots) is known for antibacterial, fungicides, and pesticide activities.^{25–27} Zhang and Rhim groups have reported the promising antibacterial effect of Sdots in recent times.^{28,29}

Received: June 25, 2022

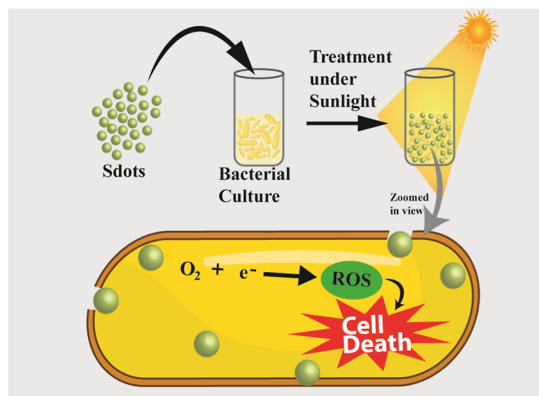
Accepted: August 31, 2022

Published: September 8, 2022



However, Sdots have not been explored as a visible light-activated antibacterial agent. Herein, we report the sunlight-activated antibacterial activity of Sdots for the first time (Scheme 1). For this purpose, we chose ampicillin-resistant *E.*

Scheme 1. Schematic Representation of the Visible Light-Driven Antibacterial Activity of Low Toxic Sdots



coli bacteria as a model system to study the antibacterial activity of the Sdots. It would be mentioned here that prevalent of antibiotic resistant is a major concern globally; thus, the recombinant bacteria used for the study provide the idea of effect of the Sdots on the resistant bacterial strains. Moreover, to check the activity of the Sdots on both Gram positive and Gram negative, we substantiated antibacterial experiments on *Bacillus subtilis* also. Furthermore, we demonstrate the excellent antibacterial activity of Sdots-fabricated polycotton fabrics, which have potential applications in personal protective masks. This approach provides the scope of use of the present materials for real-life applications like killing of pathogenic microorganism by light-activated Sdots, owing to the present pandemic scenario where personal protective kit has been in great demand. Development of Sdots fabricated polycotton will significantly prevent any secondary infection (which may be caused by settled bacteria on personal protective wear) and can make it durable as well as reusable economically.

RESULTS AND DISCUSSION

The Sdots was synthesized according to our previous report (Supporting Information, Figures S1 and S2),²⁴ and then, we thoroughly explored the photoactivated antibacterial study of the Sdots using ampicillin-resistant green fluorescence protein (GFP)-expressing recombinant *E. coli* as a model bacterium. A time-dependent study was performed to analyze the effect of the different concentrations of Sdots on bacterial growth in the presence of sunlight, dark, and standard bacterial growth conditions (SBGC) in the incubator. The bacterial growth was monitored by measuring the optical density (OD)/absorbance at 595 nm. It was observed that the Sdots were highly antibacterial in the presence of sunlight. On the other hand, to vividly understand the effect of Sdots, control experiments were also performed in the dark and in an incubator simultaneously. The experiment was conducted for 6 h duration at the temperature range of 25–38 °C in the presence of sunlight during the daytime, at around ~25 °C in the dark environment, and at 37 °C in the incubator at its standard growth environment. The minimum inhibitory concentration (MIC) of Sdots was found to be 0.16 mg/mL

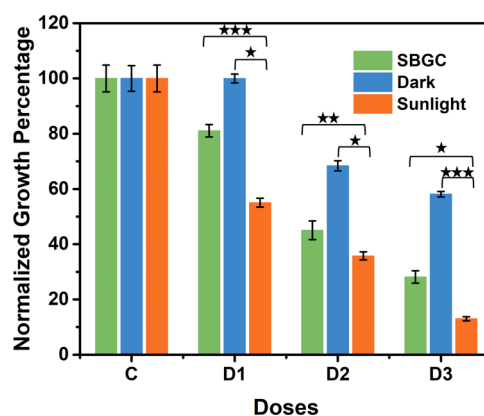


Figure 1. Normalized dose-dependent antibacterial activity measurement on *E. coli* (Gram-negative bacteria) using Sdots under SBGC, dark, and sunlight. The values are represented as mean \pm SD of results from three individual experiments. The statistical significance is denoted by \star ($p < 0.05$), $\star\star$ ($p < 0.005$), and $\star\star\star$ ($p < 0.001$).

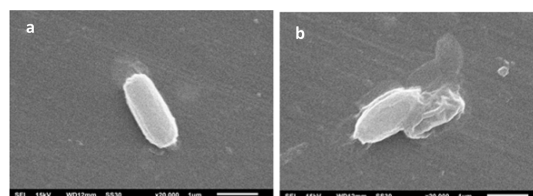


Figure 2. (a) SEM image of control bacterium showing that bacterial cell surface remained intact and healthy; (b) SEM image of treated bacterium, showing the damage in the integrity of the cell wall.

(D1), 0.56 mg/mL (D2), and 1.13 mg/mL (D3). Generally, Sdots contain a relatively less amount of sulfur than a large amount of the surface-stabilizing agent poly(ethylene glycol) (PEG).^{21–23} Therefore, the effective MIC concentration of Sdots based on the sulfur concentration is 0.01 mg/mL (D1), 0.034 mg/mL (D2), and 0.068 mg/mL (D3).^{24,32} At the abovementioned MIC concentrations, a comparative study of bacterial growth observed after 6 h under sunlight, dark, and SBGC along with the control (C) is given in Figure 1 (Figure S4, Supporting Information). In the plot, the significant inhibition of the growth in the presence of sunlight compared to SBGC is clearly observed. The percentage inhibition of the bacterial growth in the presence of sunlight was 61.63, 75.06, and 90.92% for the doses D1, D2, and D3, respectively. Similar trends were found in the *B. subtilis*, a Gram-positive bacteria cells. However, growth inhibition was found comparatively lower than the Gram-negative bacteria cells, *E. coli*. Herein, the percentage inhibition of the *B. subtilis* bacterial growth in the presence of sunlight was 16.56, 26.3, and 42.93% for the similar doses D1, D2, and D3, respectively (Figure S3). This suggests that by modifying the doses for Sdots, higher antibacterial activity can also be achieved in Gram-positive bacteria cells. Percentage deviation in bacterial growth under dark and sunlight compared with the SBGC is given in Figure S5. Comparison for the light mediated antibacterial performance in this work with previous literature reports using different materials is given in Table S1 (Supporting Information).^{35–38}

Antibacterial activity of Sdots was further studied by recording scanning electron microscopy (SEM) images to evaluate the morphological changes in the bacterial cells post-treatment of Sdots. SEM images (control bacteria group and

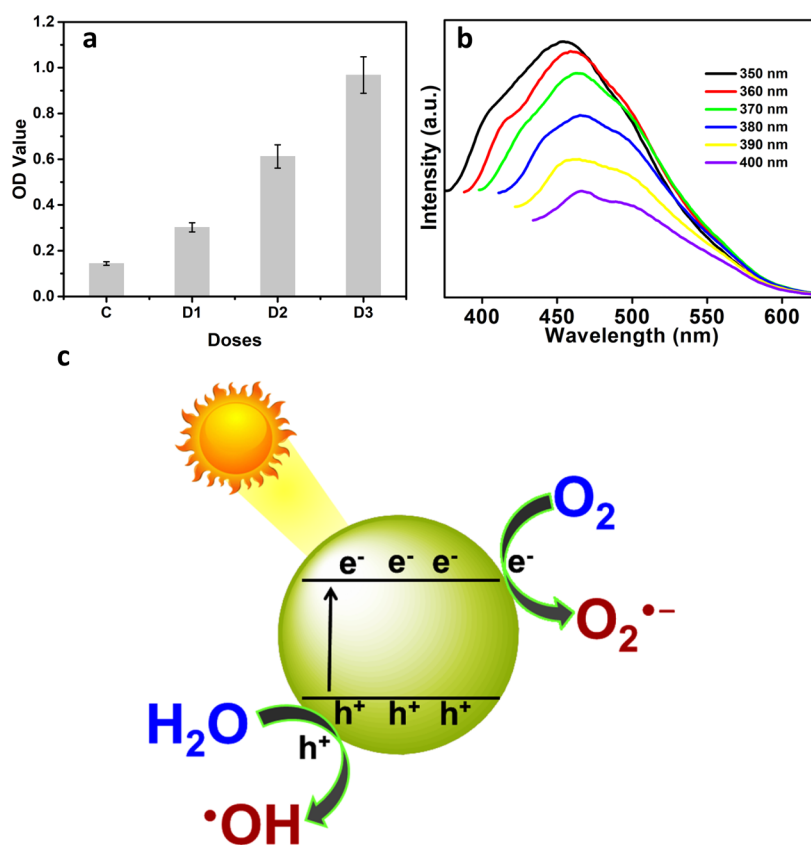


Figure 3. (a) NBT reduction test to measure the ROS generation in the presence of Sdots. The values are represented as mean \pm SD of results from three individual experiments. (b) Time-dependent fluorescence quenching of Sdots with p-BQ under visible light irradiation. Fluorescence spectra were recorded at the 365 nm excitation. (c) Schematic representation of sunlight-driven ROS generation by Sdots.

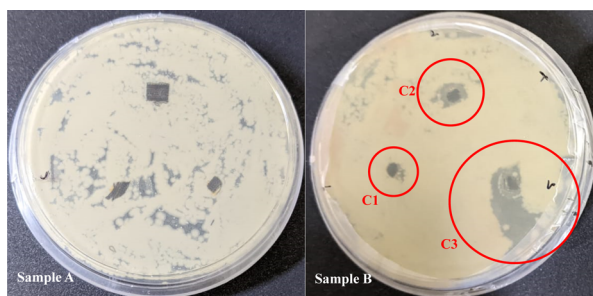


Figure 4. Antibacterial activity of Sdots-fabricated polycotton fabric for growth inhibition screening of the *E. coli* on the agar plate in the absence of Sdots (Sample A) and in the presence of Sdots (Sample B).

Sdots-treated bacteria group) indicate the strong bactericidal activity of Sdots in the presence of sunlight (Figures 2a,b and S6). The number of bacteria was decreased in the case of treated cells (Figure S6). Additionally, morphological changes can be clearly observed in the SEM images of the bacteria. The control group of bacteria showed the presence of smooth surfaces, while Sdots-treated bacteria group tended to collapse the integrity of the bacterial cell wall. This implies that the membrane integrity of the Sdots-treated bacteria was damaged in the presence of sunlight.

It has been well reported that the chemical structure of Sdots contains the polymeric sulfur core, that is, polysulfide ions (S_x^{2-}).^{21–23} Recently, the polysulfide anion was employed as an excellent visible light photoredox catalyst for organic

transformations.^{30,31} The polysulfide anion induces the reactions via single-electron transfer-driven radical-mediated processes.³⁰ Therefore, we anticipated that the generation of the ROS was one of the primary reasons for the inhibition of bacterial growth in the presence of sunlight. We carried out the nitrobluetetrazolium (NBT) reduction test to measure the ROS generation. Herein, the generation of ROS in the presence of sunlight led to the formation of formazan (blue) from the NBT (light yellow). The OD of the produced formazan from the NBT reduction method was observed at 575 nm. As shown in Figure 3a, an increased amount of OD/absorbance for doses D1, D2, and D3 confirms the ROS activity of the Sdots. The sunlight-driven photoexcited Sdots transfer the electron to the cellular oxygen and produces ROS, leading to oxidative stress in the bacteria cell. The stabilizing agent PEG in the Sdots assists in penetrating the cell wall of the bacteria. We performed time-dependent fluorescence quenching of Sdots with 1,4-benzoquinone (p-BQ) to further confirm the ROS production by Sdots under visible light irradiation.³³ p-BQ is an excellent electron acceptor and $O_2^{\bullet-}$ radical scavenger and is well studied.³³ As evident from Figure 3b, the emission intensity of Sdots (at 457 nm) is gradually decreased in the presence of p-BQ with the time duration of visible light irradiation. The fluorescence spectra were recorded at 365 nm excitation. Time-dependent UV–visible spectra of p-BQ after adding Sdots under visible light irradiation were also recorded and are presented in Figure S7 (Supporting Information). The stability of the Sdots were characterized from the absorbance plot of these Sdots, and no significant changes were observed in their stability post 1 h treatment

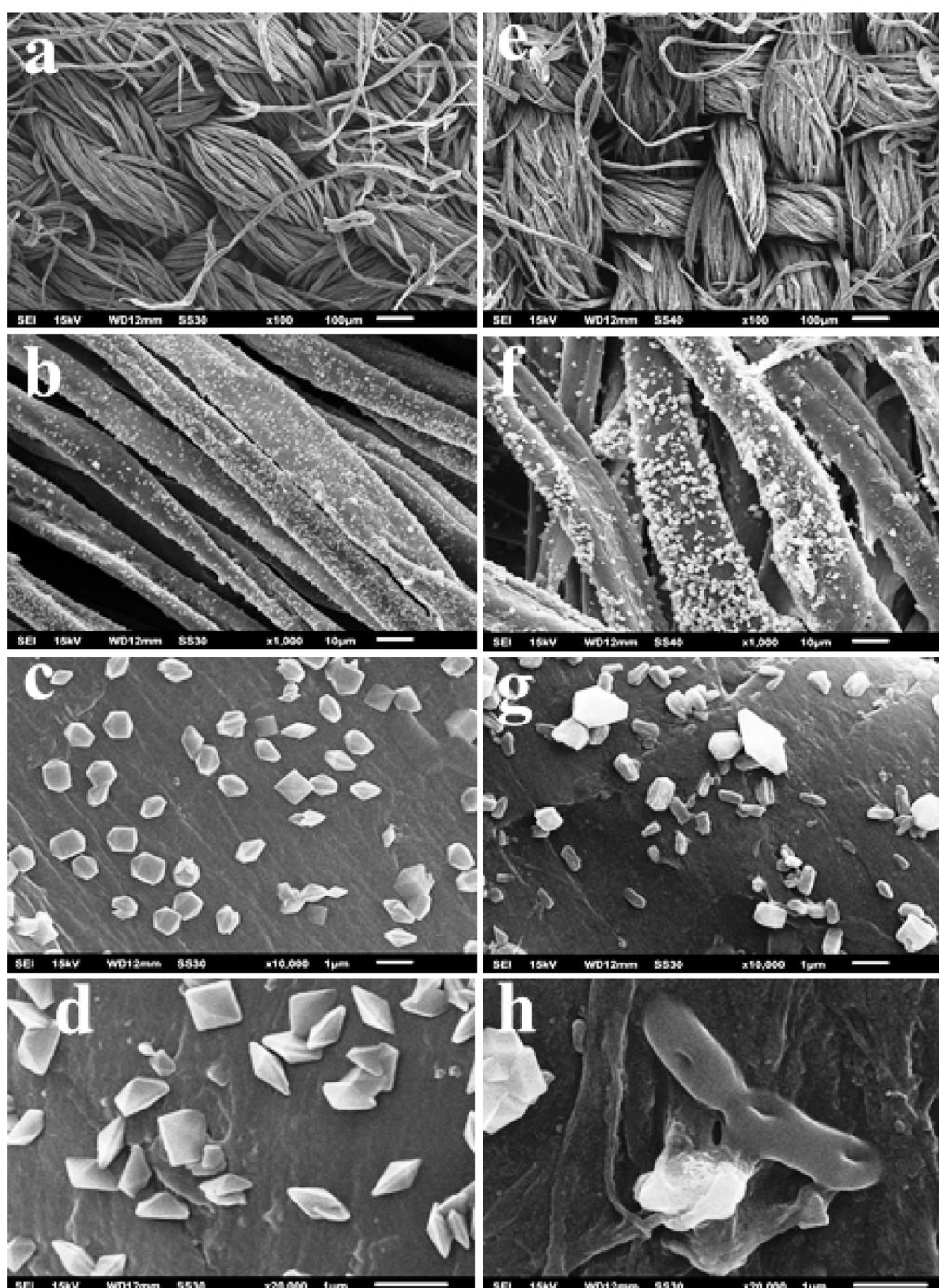


Figure 5. SEM images showing the morphology of Sdots-fabricated polycotton fabric along with its antibacterial activity. SEM images of the Sdots-fabricated polycotton fabric (a–d) and Sdots-fabricated polycotton fabric in the presence of bacteria (e–h). Scale: 100 μm (a,e), 10 μm (b,f), and 1 μm (c,d,g,h).

under sunlight (Figure S8, [Supporting Information](#)). The UV–visible spectra indicate the diminishing of the absorption peaks at 245 and 289 nm of p-BQ with the duration of visible light irradiation. Both peaks are the characteristic peak of p-BQ.^{33,34} Hence, the study further revealed the formation of photo-excited electrons of Sdots and the subsequent scavenging of $\text{O}_2^{\bullet-}$ radical by the p-BQ.^{33,34} The schematic representation of ROS generation by Sdots under sunlight is given in [Figure 3c](#).^{35,36}

The practicality of the Sdots as photoactivated antibacterial agents was further explored for the development of

antibacterial fabric. For this purpose, we used polycotton fabric for growth inhibition screening of the *E. coli* on an agar plate in the presence and absence of Sdots. The post-incubation results in the absence (Sample A) and presence (Sample B) of Sdots are shown in [Figure 4](#). The growth differences of the bacterial colony can be clearly visualized through the zone of inhibition in sample B. Three different concentrations C1 (10 μL), C2 (20 μL), and C3 (30 μL) of the Sdots (20 mg/mL) were applied to the polycotton. The Sdots amount coated on polycotton at different doses applied is given in [Table S2](#) ([Supporting Information](#)). These concen-

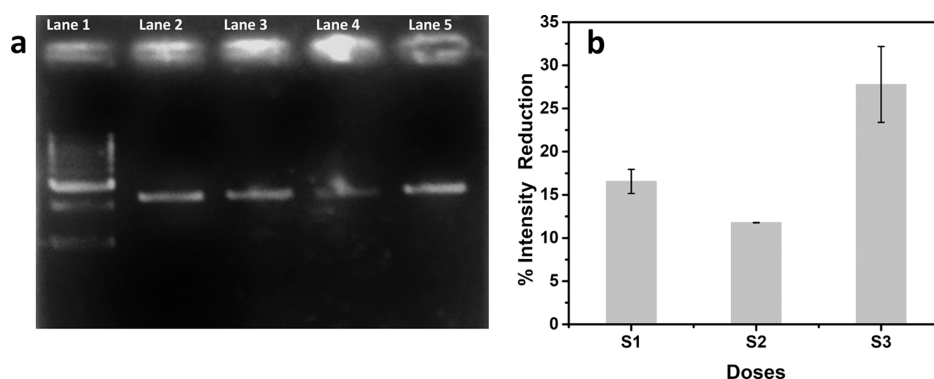


Figure 6. (a) DNA-binding assay: Lane 1—ladder DNA, lane 2–4—varying concentration of Sdots [L2: S1(4 mg/mL), L3: S2(8 mg/mL), and L4: S3(12 mg/mL)], and lane 5—control pDNA. The gel microgram shows no significant change in the band pattern in S1 and S2, whereas slight lesser migration of the pDNA is shown in S3; (b) showing percentage reduction of pixel intensity of S1, S2, and S3 in comparison with control. The values are represented as mean \pm SD of results from three individual experiments.

trations were taken based on the Sdots retention capacity (RC) of the fabric, which is below RC (C1), at RC (C2), and above RC (C3). Herein, the higher antibacterial activity was confirmed by the increasing zone of inhibition sizes for C1, C2, and C3, which are 2 ± 0.5 , 4 ± 1.5 , and 9 ± 4 mm, respectively. The increased concentration of the Sdots showed more potent antibacterial activity that can be visualized in C3 of sample B, where excess Sdots spilled from the fabric distinctively restricted the growth of the bacterial colony.

The morphology of these polycotton fabrics was further studied by SEM. In Figure 5, SEM images of the Sdots-treated polycotton fabric in the presence and absence of the bacteria are given. It would be mentioned here that individual Sdots would not be visible under SEM with this magnification that was visible in TEM analysis. The polygonal structure (due to aggregates of Sdots) confirms the uniform distribution of the Sdots over the polycotton fabrics (Figure 5b,f). The average size was 188 ± 56 nm. Furthermore, SEM images of different magnifications also demonstrate the integrity of the interwoven threads of the polycotton as no damage to this thread can be observed in higher magnification (Figure 5a–h). However, in the presence of bacteria, the antibacterial activity of these Sdots was prominent as dead/damaged bacteria were seen (Figure 5g–h).

Furthermore, to know the interaction of the Sdots at the molecular level, we studied the interactions of Sdots with plasmid DNA (pDNA) isolated from GFP expressing recombinant *E. coli*. Different concentrations of Sdots, such as S1(4 mg/mL), S2(8 mg/mL), and S3(12 mg/mL), were added to the pDNA, followed by gel agarose electrophoresis. The results are given in Figure 6a,b, showing no significant change in the band pattern of the pDNA. However, at higher concentrations of Sdots, $\sim 27\%$ reduction in the band intensity of pDNA was observed, possibly due to the non-covalent interactions with the Sdots. Thus, the gel electrophoresis study revealed a weak interaction of the pDNA with Sdots.

CONCLUSIONS

In conclusion, we have explored the visible light-activated antibacterial activity of water soluble Sdots for the first time. Sdots exhibited antibacterial activity by generating ROS under sunlight as photoexcited Sdots transfer the electron to the cellular oxygen. Notably, the low toxicity (or cytotoxicity) of Sdots is a significant advantage for translational applications. Hence, the excellent photoactivated bactericidal activity of

Sdots was further employed for cleaning the bacterial infection on the Sdots-coated polycotton fabrics, which have potential applications in self-disinfection personal protective masks. This work might provide a new prospect for the development of Sdots-based photodynamic antimicrobial chemotherapy and photocatalytic disinfection in diverse locations of interest.

ASSOCIATED CONTENT

Supporting Information

The Supporting Information is available free of charge at <https://pubs.acs.org/doi/10.1021/acsomega.2c03968>.

Experiments, excitation wavelength-dependent emission spectra of Sdots, TEM analysis revealing the formation of Sdots, normalized dose-dependent antibacterial activity measurement, dose-dependent antibacterial activity measurement, percentage reduction of bacterial growth in a control sample, SEM image of control bacteria and treated bacteria, comparison for the antibacterial performance in this work with previous literature reports, time-dependent UV–visible spectra of p-BQ after adding Sdots under visible light irradiation, half diluted UV–visible spectra of p-BQ and Sdots, comparison of the absorbance plot of the Sdots original sample with the sunlight-treated Sdots sample, and Sdots amount coated on polycotton at different doses (PDF)

AUTHOR INFORMATION

Corresponding Authors

Md Palashuddin Sk – Department of Chemistry, Aligarh Muslim University, Aligarh 202002 Uttar Pradesh, India; orcid.org/0000-0003-2330-7382; Phone: (+91) 0571-2700920 ext-3386; Email: palashuddin.ch@amu.ac.in

Amaresh Kumar Sahoo – Department of Applied Sciences, Indian Institute of Information Technology Allahabad, Prayagraj 211012 Uttar Pradesh, India; orcid.org/0000-0002-9014-3317; Email: asahoo@iiita.ac.in

Authors

Saurabh Shivalkar – Department of Applied Sciences, Indian Institute of Information Technology Allahabad, Prayagraj 211012 Uttar Pradesh, India; orcid.org/0000-0002-7912-1627

Farwa Arshad – Department of Chemistry, Aligarh Muslim University, Aligarh 202002 Uttar Pradesh, India

Complete contact information is available at:
<https://pubs.acs.org/10.1021/acsomega.2c03968>

Author Contributions

S.S. and F.A. contributed equally. S.S. conducted all the antibacterial experiments and prepared the manuscript. F.A. synthesized and characterized Sdots. A.K.S. designed the experiments, analyzed the data, and carried out the reviewing and editing of the manuscript. M.P.S. conceptualized, designed the experiments, analyzed the data, and carried out the writing and reviewing the manuscript.

Notes

The authors declare no competing financial interest.

ACKNOWLEDGMENTS

M.P.S. and F.A. acknowledge the Department of Chemistry, Aligarh Muslim University (AMU), for providing instrumental facility. The authors acknowledge University Sophisticated Instrument Facility (USIF), AMU, Aligarh. S.S. and A.K.S. acknowledge the Department of Applied Sciences, Indian Institute of Information Technology, Allahabad, for providing instrumental facility. Neelima Varshney is acknowledged for her help.

ABBREVIATIONS

ROS, reactive oxygen species; Sdots, sulfur dots; Cdots, carbon dots; GFP, green fluorescence protein; SBGC, standard bacterial growth conditions; OD, optical density; SET, single electron driven; SEM, scanning electron microscopy; NBT, nitrobluetetrazolium; *p*-BQ, 1,4-benzoquinone; pDNA, plasmid DNA

REFERENCES

- (1) Zhou, Z.; Li, B.; Liu, X.; Li, Z.; Zhu, S.; Liang, Y.; Cui, Z.; Wu, S. Recent Progress in Photocatalytic Antibacterial. *ACS Appl. Bio Mater.* **2021**, *4*, 3909–3936.
- (2) Crofts, T. S.; Gasparrini, A. J.; Dantas, G. Next-Generation Approaches to Understand and Combat the Antibiotic Resistome. *Nat. Rev. Microbiol.* **2017**, *15*, 422–434.
- (3) O'Neil, J. Health Wealth Nations, 2014; pp 1–16. https://amr-review.org/sites/default/files/AMR%20Review%20Paper%20-%20Tackling%20a%20crisis%20for%20the%20health%20and%20wealth%20of%20nations_1.pdf (accessed Jun 25, 2022).
- (4) Kumar, R.; Anandan, S.; Hembram, K.; Narasinga Rao, T. Efficient ZnO-Based Visible-Light-Driven Photocatalyst for Antibacterial Applications. *ACS Appl. Mater. Interfaces* **2014**, *6*, 13138–13148.
- (5) Yadav, H. M.; Kim, J.-S.; Pawar, S. H. Developments in Photocatalytic Antibacterial Activity of Nano TiO₂: A Review. *Korean J. Chem. Eng.* **2016**, *33*, 1989–1998.
- (6) Ren, Y.; Liu, H.; Liu, X.; Zheng, Y.; Li, Z.; Li, C.; Yeung, K. W. K.; Zhu, S.; Liang, Y.; Cui, Z.; Wu, S. Photoresponsive Materials for Antibacterial Applications. *Cell Rep. Phys. Sci.* **2020**, *1*, 100245.
- (7) Sun, L.; Du, T.; Hu, C.; Chen, J.; Lu, J.; Lu, Z.; Han, H. Antibacterial Activity of Graphene Oxide/g-C₃N₄ Composite through Photocatalytic Disinfection under Visible Light. *ACS Sustainable Chem. Eng.* **2017**, *5*, 8693–8701.
- (8) Zhao, Y.; Jia, Y.; Xu, J.; Han, L.; He, F.; Jiang, X. The Antibacterial Activities of MoS₂ Nanosheets towards Multi-Drug Resistant Bacteria. *Chem. Commun.* **2021**, *57*, 2998–3001.
- (9) Dong, X.; Liang, W.; Meziani, M. J.; Sun, Y.-P.; Yang, L. Carbon Dots as Potent Antimicrobial Agents. *Theranostics* **2020**, *10*, 671–686.
- (10) Wellia, D. V.; Kusumawati, Y.; Diguna, L. J.; Amal, M. I. Introduction of Nanomaterials for Photocatalysis. In *Nanocomposites for Visible Light-Induced Photocatalysis*; Khan, M. M., Pradhan, D., Sohn, Y., Eds.; Springer Series on Polymer and Composite Materials; Springer International Publishing: Cham, 2017; pp 1–17.
- (11) Rahman, A.; Tan, A. L.; Harunsani, M. H.; Ahmad, N.; Hojamberdiev, M.; Khan, M. M. Visible Light Induced Antibacterial and Antioxidant Studies of ZnO and Cu-Doped ZnO Fabricated Using Aqueous Leaf Extract of Ziziphus Mauritiana Lam. *J. Environ. Chem. Eng.* **2021**, *9*, 105481.
- (12) Rahman, A.; Khan, M. M. Chalcogenides as Photocatalysts. *New J. Chem.* **2021**, *45*, 19622–19635.
- (13) Bottrill, M.; Green, M. Some Aspects of Quantum Dot Toxicity. *Chem. Commun.* **2011**, *47*, 7039–7050.
- (14) Wang, D.; Lin, Z.; Wang, T.; Yao, Z.; Qin, M.; Zheng, S.; Lu, W. Where Does the Toxicity of Metal Oxide Nanoparticles Come from: The Nanoparticles, the Ions, or a Combination of Both? *J. Hazard. Mater.* **2016**, *308*, 328–334.
- (15) Rahman, A.; Harunsani, M. H.; Tan, A. L.; Ahmad, N.; Min, B.-K.; Khan, M. M. Influence of Mg and Cu Dual-Doping on Phytochemical Synthesized ZnO for Light Induced Antibacterial and Radical Scavenging Activities. *Mater. Sci. Semicond. Process.* **2021**, *128*, 105761.
- (16) Muslih, E. Y.; Munir, B.; Khan, M. M. 2 - Advances in Chalcogenides and Chalcogenides-Based Nanomaterials Such as Sulfides, Selenides, and Tellurides. In *Chalcogenide-Based Nanomaterials as Photocatalysts*; Khan, M. M., Ed.; Micro and Nano Technologies; Elsevier, 2021; pp 7–31.
- (17) Lam, S.-M.; Sin, J.-C.; Zeng, H.; Lin, H.; Li, H.; Qin, Z.; Lim, J. W.; Mohamed, A. R. Z-Scheme MoO₃ Anchored-Hexagonal Rod like ZnO/Zn Photoanode for Effective Wastewater Treatment, Copper Reduction Accompanied with Electricity Production in Sunlight-Powered Photocatalytic Fuel Cell. *Sep. Purif. Technol.* **2021**, *265*, 118495.
- (18) Lam, S.-M.; Sin, J.-C.; Lin, H.; Li, H.; Lim, J. W.; Zeng, H. A Z-Scheme WO₃ Loaded-Hexagonal Rod-like ZnO/Zn Photocatalytic Fuel Cell for Chemical Energy Recuperation from Food Wastewater Treatment. *Appl. Surf. Sci.* **2020**, *514*, 145945.
- (19) Lam, S.-M.; Chew, K.-C.; Sin, J.-C.; Zeng, H.; Lin, H.; Li, H.; Lim, J. W.; Mohamed, A. R. Ameliorated Photodegradation Performance of Polyethylene and Polystyrene Films Incorporated with ZnO-PVP Catalyst. *J. Environ. Chem. Eng.* **2022**, *10*, 107594.
- (20) Knoblauch, R.; Geddes, C. D. Carbon Nanodots in Photodynamic Antimicrobial Therapy: A Review. *Materials* **2020**, *13*, 4004.
- (21) Shi, Y.; Zhang, P.; Yang, D.; Wang, Z. Synthesis, Photoluminescence Properties and Sensing Applications of Luminescent Sulfur Nanodots. *Chem. Commun.* **2020**, *56*, 10982–10988.
- (22) Ruan, H.; Zhou, L. Synthesis of Fluorescent Sulfur Quantum Dots for Bioimaging and Biosensing. *Front. Bioeng. Biotechnol.* **2022**, *10*, 909727.
- (23) Pal, A.; Arshad, F. Emergence of Sulfur Quantum Dots: Unfolding Their Synthesis, Properties, and Applications. *Adv. Colloid Interface Sci.* **2020**, *285*, 102274.
- (24) Arshad, F.; Sk, M. P.; Maurya, S. K.; Siddique, H. R. Mechanochemical Synthesis of Sulfur Quantum Dots for Cellular Imaging. *ACS Appl. Nano Mater.* **2021**, *4*, 3339–3344.
- (25) Schneider, T.; Baldauf, A.; Ba, L. A.; Jamier, V.; Khairan, K.; Sarakbi, M.-B.; Reum, N.; Schneider, M.; Röseler, A.; Becker, K.; Burkholz, T.; Winyard, P. G.; Kelkel, M.; Diederich, M.; Jacob, C. Selective Antimicrobial Activity Associated with Sulfur Nanoparticles. *J. Biomed. Nanotechnol.* **2011**, *7*, 395–405.
- (26) Rao, K. J.; Paria, S. Use of Sulfur Nanoparticles as a Green Pesticide on Fusarium Solani and Venturia Inaequalis Phytopathogens. *RSC Adv.* **2013**, *3*, 10471–10478.
- (27) Griffith, C. M.; Woodrow, J. E.; Seiber, J. N. Environmental Behavior and Analysis of Agricultural Sulfur. *Pest Manage. Sci.* **2015**, *71*, 1486–1496.
- (28) Wang, Y.; Zhao, Y.; Wu, J.; Li, M.; Tan, J.; Fu, W.; Tang, H.; Zhang, P. Negatively Charged Sulfur Quantum Dots for Treatment of Drug-Resistant Pathogenic Bacterial Infections. *Nano Lett.* **2021**, *21*, 9433–9441.

- (29) Priyadarshi, R.; Riahi, Z.; Rhim, J.-W.; Han, S.; Lee, S.-G. Sulfur Quantum Dots as Fillers in Gelatin/Agar-Based Functional Food Packaging Films. *ACS Appl. Nano Mater.* **2021**, *4*, 14292–14302.
- (30) Li, H.; Tang, X.; Pang, J. H.; Wu, X.; Yeow, E. K. L.; Wu, J.; Chiba, S. Polysulfide Anions as Visible Light Photoredox Catalysts for Aryl Cross-Couplings. *J. Am. Chem. Soc.* **2021**, *143*, 481–487.
- (31) Steudel, R.; Chivers, T. The Role of Polysulfide Dianions and Radical Anions in the Chemical, Physical and Biological Sciences, Including Sulfur-Based Batteries. *Chem. Soc. Rev.* **2019**, *48*, 3279–3319.
- (32) Arshad, F.; Sk, M. P. Luminescent Sulfur Quantum Dots for Colorimetric Discrimination of Multiple Metal Ions. *ACS Appl. Nano Mater.* **2020**, *3*, 3044–3049.
- (33) Bhunia, S.; Ghorai, N.; Burai, S.; Purkayastha, P.; Ghosh, H. N.; Mondal, S. Unraveling the Carrier Dynamics and Photocatalytic Pathway in Carbon Dots and Pollutants of Wastewater System. *J. Phys. Chem. C* **2021**, *125*, 27252–27259.
- (34) Verma, A.; Shivalkar, S.; Sk, M. P.; Samanta, S. K.; Sahoo, A. K. Nanocomposite of Ag Nanoparticles and Catalytic Fluorescent Carbon Dots for Synergistic Bactericidal Activity through Enhanced Reactive Oxygen Species Generation. *Nanotechnology* **2020**, *31*, 405704.
- (35) Lam, S.-M.; Sin, J.-C.; Zeng, H.; Lin, H.; Li, H.; Chai, Y.-Y.; Choong, M.-K.; Mohamed, A. R. Green Synthesis of Fe-ZnO Nanoparticles with Improved Sunlight Photocatalytic Performance for Polyethylene Film Deterioration and Bacterial Inactivation. *Mater. Sci. Semicond. Process.* **2021**, *123*, 105574.
- (36) Lam, S.-M.; Sin, J.-C.; Lin, H.; Li, H.; Zeng, H. Greywater and Bacteria Removal with Synchronized Energy Production in Photocatalytic Fuel Cell Based on Anodic TiO₂/ZnO/Zn and Cathodic CuO/Cu. *Chemosphere* **2020**, *245*, 125565.
- (37) He, W.; Kim, H.-K.; Wamer, W. G.; Melka, D.; Callahan, J. H.; Yin, J.-J. Photogenerated Charge Carriers and Reactive Oxygen Species in ZnO/Au Hybrid Nanostructures with Enhanced Photocatalytic and Antibacterial Activity. *J. Am. Chem. Soc.* **2014**, *136*, 750–757.
- (38) Fakhri, A.; Kahi, D. S. Synthesis and Characterization of MnS₂/Reduced Graphene Oxide Nanohybrids for with Photocatalytic and Antibacterial Activity. *J. Photochem. Photobiol., B* **2017**, *166*, 259–263.